Preparation, Characterization and Visible Light Photocatalytic Activities of Samarium-Doped Mixed Crystalline Phase TiO_2 Nanoparticles

IOP Conf. Series: Materials Science and Engineering **562** (2019) 012031 doi:10.1088/1757-899X/562/1/012031

Preparation, Characterization and Visible Light Photocatalytic Activities of Samarium-Doped Mixed Crystalline Phase TiO_2 Nanoparticles

Fuchang Peng[1,2*], Qi Lai[1,2], Wei Chang[3] and Yan Cui[2]
1. School of Vanadium & Titanium,
2. Panzhihua Graphene Engineering Technology Research Center,
3. School of foreign languages, Panzhihua University, 10 Airport Road, Panzhihua, 617000, PR China
E-mail: pzhupfc@163.com

Abstract. Mixed crystalline phase TiO_2 nanoparticles with different content of Sm ion were prepared by a facile sol-gel method. The samples were characterized by XRD, XPS, UV-Vis-DRS, and PL. The influence of Sm-doping on structure and visible light photocatalytic activity of mixed phase TiO_2 was evaluated by photocatalytic degradation of MB under the irradiation of fluorescent lamp. The results indicate that samarium appears two kinds of Sm^{3+} and Sm^{2+} valence state on the surface of TiO_2. Sm doping can restrain the phase transition from anatase to rutile, and prevent the grain growth. Appropriate amount of Sm doping and the proportions of rutile and anatase mixed phase can effectively inhibit the recombination of photo-generated electron and hole pairs, expand the wavelength range of absorption spectrum. Moreover, the photocatalytic activity of Sm-TiO_2 in MB degradation is evidently enhanced. The MB degradation rate of Sm-TiO_2 samples with n(Sm): n(Ti)=0.006 is the best under the irradiation of fluorescent light when the sintered temperature T=500°C, it is 97% within 6 h, which is significantly higher than 56.4% of pure TiO_2 under the same experimental conditions.

1. Introduction

Environment pollution and destruction on the global scale are issues of increasing concern in today's society. There is a need for effective catalysts for the degradation of polltants. Photocatalytic reaction is a green technology driven by light irradiation. Solar-driven chemical reaction at room temperature has an important application prospect in the field of Environmental protection and clean energy production [1,2]. Titanium doxide (TiO_2) nanostructures have attracted interest due to their stable chemical properties, low cost, clean, non-toxic properties and potential apoplication in environmental treatment, solar cells, photocatalytic decomposition of aquatic hydrogen production and other fields [3,4]. It is a promising environmental-friendly photocatalytic material. However, the band gap of anatase TiO_2 is about 3.2 eV, which make it only be excited by ultraviolet light (λ<387 nm), so that its utilization of solar light is low in practical applications. Moreover, photogenerated electron-hole pairs of TiO_2 are easily recombined during migration, which greatly reduces the efficiency of TiO_2 quantum conversion. These factors seriously restrict the actual application scope and scale of TiO_2 photocatalyst.

Recent years, modification methods of TiO_2 have been extensively studied at home and abroad, such as ion doping, precious metal deposition, semiconductor compounding and dye sensitization. The band structure and surface state of TiO_2 have been adjusted, the visible light absorption has been enhanced, and the recombination probability of photogenerated electron-hole pairs has been reduced

through various modifications [5]. Generally, among various methods, doping TiO_2 with rare earth metals ions were reported as a good approach to improve the photocatalytic performance. Because the valence electron layer of rare earth elements ($4f^n6s^2$ or $4f^{n-1}5d^16s^2$) is a special 4*f* electronic structure, which has abundant energy levels and is easy to produce multi-electron configuration. The rare earth oxides are characterized by good thermal stability and strong selective adsorption [6]. So the doping of rare earth metal ions are considered as an important modification way to improve the photocatalytic activity of TiO_2 [7,8]. Rare earth ions doped into the lattice of TiO_2 can form electron traps, promote photogenerated electron-hole pairs separation and improve photocatalytic activity [9]. In addition, rare earth ions can help to concentrate organic pollutants adsorbed on the surface of the catalyst and enhance the photocatalytic sensitivity of the catalyst [10]. Up to now, there have been many reports on the experimental results of photocatalytic activity of rare earth metal ions doped TiO_2 [11]. However, the effect of Sm doping on the structure and visible-light photocatalytic activity of mixed crystalline TiO_2 and its mechanism are less studied. Therefore, it is still of great significance to study the effect of rare earth ions on the microstructure and photocatalytic activity of mixed-phase nano-TiO_2.In this paper, a simple aqueous sol-gel method was used to synthesize mixed crystalline phase nano-TiO_2 with different Sm doping content. In this paper, Sm-TiO_2 samples were synthesized and characterized, and the effects of Sm doping on its structure and visible-light photocatalytic activity were studied.

2. Experiment

The solution A was obtained by mixing deionized water and hydrolysis inhibitor in a certain proportion in a water bath at 60°C. At the same time, 5 mL tetrabutyl titanate (CP) was slowly dripped into solution A and mixed solution B was obtained. $Sm(NO_3)_3{\cdot}6H_2O$(Aladdin Industrial Company, AP) with different content was calculated and weighed by the mole ratio of Sm/Ti. After dissolving in 5 mL deionized water, $Sm(NO_3)_3{\cdot}6H_2O$ was slowly dripped into B. The pH value of the solution was adjusted to 2~3 by 2.5 mol/L nitric acid. The solution was stirred continuously for 12~16 hours to form a uniform yellowish sol. The Sm-TiO_2 nanoparticles were obtained after aging, drying, roasting and grinding. The above experimental steps were repeated to prepare undoped pure TiO_2 samples.

Phase analysis was carried out by X ray diffractometer (TTRIII target). The particle size distribution of samples was characterized of by nano-sizer (Malvern Company). The valence state of the elements was analyzed by X ray photoelectron spectroscopy (XSAM800). The UV-Vis diffuse reflectance spectra of samples were analyzed by spectrophotometer (U-4100). The fluorescence spectra were analyzed by fluorescence spectrophotometer (FL4500). Absorbance determination was measured by visible spectrophotometer (722N).

The photodegradation activities of the Sm-TiO_2 samples on methylene blue (MB) solutions were studied under the irradiation of fluorescent light. The suspension was formed by adding 0.20 g TiO_2 catalyst sample into 50 mL MB solution (mass concentration ρ=10 mg/L) and stirring for 40 min in dark condition to make the adsorption-desorption equilibrium. The suspension was placed in a 30 W Philips fluorescent lamp to simulate the visible light source and reacted. MB Samples were taken at intervals of 1 h for 4 mL. After centrifugal separation of the MB sample with 3500 r/min and 40 min·per times, the absorbance values of the supernatant at 664 nm wavelength were determined. The degradation rate of MB was expressed by equation(1).

$$\eta(\%) = \frac{A_0 - A_t}{A_0} \times 100\% \quad (1)$$

where η is the photo-degradation conastant of MB, t is the reaction time, A_0 and A_t are the initial and remnant MB concertration , respectively.

3. Results and Discussion

3.1. X-ray Diffraction

In order to study the effect of samarium doping on the crystal structure of titanium dioxide, the XRD patterns of Sm-TiO_2 samples sinted at 500°C were analyzed, as shown in Figure 1. The results indicate that all the samples are mixed crystal phases composed of anatase and rutile. Strong diffraction peaks

of the samples indicated the high crystallinity of the samples. The diffraction peaks in the diagram can be attributed to the characteristic peaks of the phase structure of anatase or rutile. There is no characteristic peak of Sm and its oxides in the doped samples. It may be that Sm ions are highly dispersed in the microcrystalline gap of nano-TiO_2 in the form of amorphous oxides, or Sm doping amount is too low to be detected by the instrument.

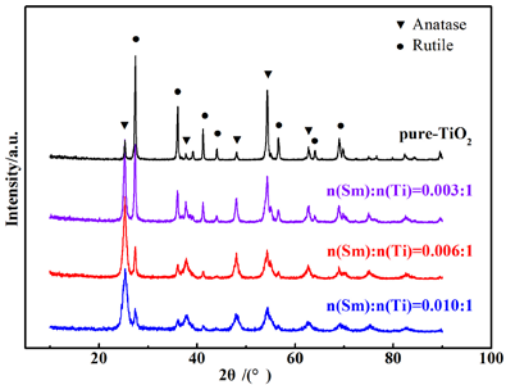

Figure 1. XRD patterns of TiO_2 samples doped with different Sm contents at 500°C.

Usually, the phase content, average grain size, lattice distortion and specific surface area of TiO_2 can be estimated from XRD data [12]. According to the characteristic peaks of anatase phase (2θ=25.28°) and rutile phase (2θ=27.45°) in the XRD spectrum of titanium dioxide, the content of anatase phase was calculated by Qantitative formula. The average grain size was calculated by Scherrer formula. Anatase content and crystalline size are shown in Table 1. It can be seen that the content of anatase phase and grain size of Sm-TiO_2 samples show regular changes. With increasing the samarium doping concentration, he content of anatase phase in the samples increases gradually. The diffraction peak broadens obviously. Meanwhile, the average grain size decreases gradually with the increase of Sm content. These results indicate that Sm ion doping inhibits the phase transition from anatase to rutile and refines the grain size of TiO_2. The phase transformation and grain growth of nano TiO_2 are hindered by the synergistic rearrangement of Ti and O atoms during heat treatment.

Table 1. Anatase content and average crystalline size of different TiO_2 nanoparticles at 500 °C

Samples	Content of anatase phase (%)	Average crystal size(nm)	
n(Sm): *n*(Ti)		D_A/nm	D_R/nm
pure TiO_2	12.4	29.8	32.1
0.003: 1	45.6	18.6	25.6
0.006: 1	68.7	14.5	22.7
0.010: 1	73.6	10.4	19.0

3.2. XPS Analysis

XPS analysis was performed to examine the surface chemical states and content of foreign dopant and intrinsic ions in the Sm-TiO_2 sample, which was calcined at 500 °C. The XPS results are shown in Figure 2. Figure 2(a) shows the XPS full spectrum of Sm-TiO_2 sample. It can be found that the surface of the doped sample is composed of Ti, O, Sm and a trace amount of carbon. The Ti, O, Sm elements result from the Sm-TiO_2 sample and element carbon mey be attributed to the calcination process or the oil pollution from XPS instrument itself.

Figure 2(b), (c) and (d) are high-resolution XPS spectrum of Ti 2p, O 1s and Sm 3d respectively. In the Ti 2p high-resolution XPS spectrum (Figure 2(b)), two peaks belong to Ti 2p1/2 and Ti 2p3/2. These peaks were attributed to Ti^{4+} and were similar to those of P25(Ti 2p3/2 458.5 eV and Ti 2p1/2 464.2 eV)[13]. In Figure 2(c), the strong peak at 529.3 eV is consistent with the O 1s characteristic

peak of TiO_2, which is the vacancy oxygen in TiO_2. In Figure 2(d), the binding energies at 1108 eV and 1072.9 eV belong to Sm 3d3/2 and Sm 3d5/2 respectively, both of which are related to the bond energies of Sm 3d in Sm_2O_3, while the weak peaks at 1083.9 eV originate from the contribution of Sm^{2+} [14], which may be due to the formation of Sm-O-Ti bonds on the surface of TiO_2. The above results show that there are two kinds of samarium species of Sm^{2+} and Sm^{3+} on the surface of TiO_2 after Sm doping. Sm^{3+} species can easily capture electrons and be reduced to Sm^{2+} in the process of photocatalytic reaction. However, unstable Sm^{2+} species can easily lose electrons. The transferred electrons interact with $\cdot O_2$ adsorbed on the surface of the catalyst to form strongly oxidizing superoxide radical O_2^- [15]. It is through this cycle that the photogenerated electron-hole pairs are separated and valence bands are promoted. The formed hole is also a highly oxidizing group, which can effectively oxidize organic molecules and ultimately improve the photocatalytic activity [16].

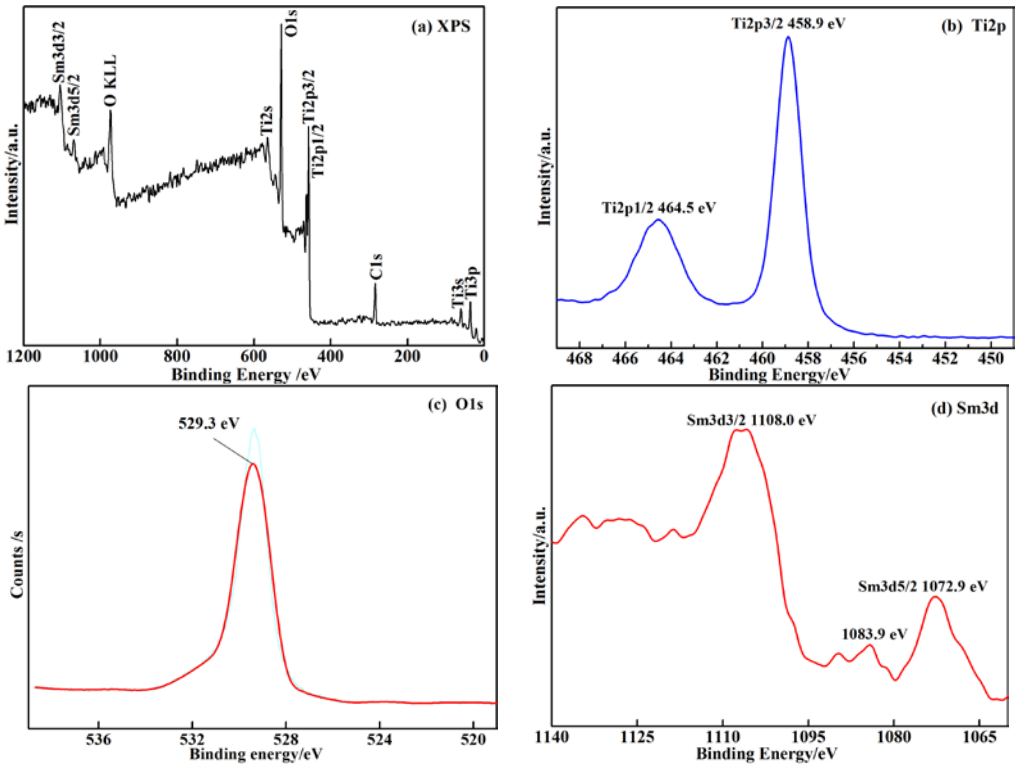

Figure 2. XPS spectra of Sm-TiO_2 samples with *n*(Sm): *n*(Ti)=0.006.

3.3. UV-Vis-DRS and PL Spectra Analysis

Figure 3(a) demonstrates the UV-Vis-DRS spectrum of different TiO_2 samples calcined at 500°C. It is obvious that pure TiO_2 only absorbs UV light, while there is an obvious red-shift in Sm-TiO_2 samples and it increases with the increasing Sm ion doping concentration. Among all the samples, the largest red-shift can be found in Sm-TiO_2 samples with *n*(Sm): *n*(Ti)=0.006. The absorption of Sm-TiO_2 samples was enhanced, and continuous absorption occurs in the visible region. The absorption band edge is red-shifted from 408 nm to 418 nm. The band gap is calculated by the formula as equation(2).[17]

$$E_g(eV) = \frac{1240}{\lambda(nm)} \quad (2)$$

The band gap of TiO_2 decreases from 3.04 eV to 2.97 eV before and after doping. The results of XRD analysis show that the main phase of TiO_2 before doping is rutile phase, and the forbidden band is narrower than anatase phase. The influence of rare earth doping on the absorption of light is due to the introduction of new impurity level above Fermi level, crystal defect caused by doping and the contribution of 4*f* electron transition [18]. Samarium doping broadens the absorption spectrum of TiO_2. In addition, the electron in the O 2p orbital of the doped sample will absorb certain energy photons and

then transit to the Sm 3d orbital, which will produce an absorption band between 300 and 500 nm, further improving the utilization of visible light.

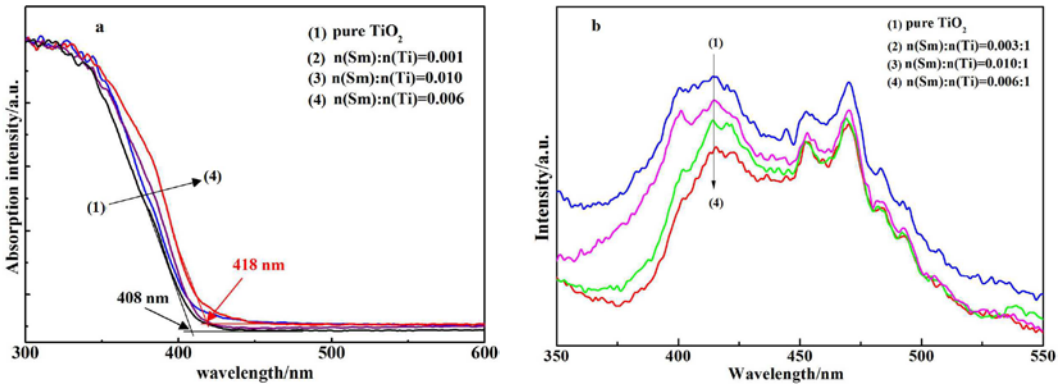

Figure 3. (a) UV-Vis-DRS spectra and (b) Photoluminescence spectra of Sm-TiO_2 samples with different Sm doping concentration.

The PL emission spectra of Sm-TiO_2 samples was to disclose the separation efficiency of photo-electron-hole pairs. Figure 3(b) shows the PL of Sm-TiO_2 samples with different Sm doping amoun when the excitation wavelength is 300nm. Two main emission peaks at 400~500 nm are found in Figure 3(b), which show strong and wide emission signals. These spectral signals are related to the defects of nanoparticles and surface oxygen vacancies. The peak at 410 nm is the band-edge free exciton luminescence, while the peak at 470 nm is the bound exciton luminescence [19]. The PL spectral lines of all samples are basically the same, which indicates that there is no new fluorescence phenomenon in Sm-TiO_2, but the PL spectral intensity has changed. Namely, Sm doping affects the fluorescence spectral intensity. The results show that the impurity level introduced by rare earth doped TiO_2 can be used as a shallow trap for photogenerated electrons [20], and the photogenerated electron-hole pairs recombination can be effectively inhibited by adding appropriate Sm ions. When n(Sm): n(Ti)=0.006, the PL strength of Sm-TiO_2 is the weakest, which indicates that the photogenerated electron-hole pairs recombination probability is the lowest and the quantum efficiency is the highest. These results can be confirmed by the subsequent photocatalytic activity test results.

3.4. Photodegradation Activity on MB and Reaction Mechanism

The effect of photocatalytic degradation of MB over different TiO_2 samples are shown in Figure 4. It can be seen that the properties of Sm-TiO_2 samples are significantly higher than those of pure TiO_2 samples. With prolonging the illumination time, the photodegradation percentages of MB over the series of TiO_2 catalysts increase gradually and reach 97% at 6 h for the best catalyst. The photodegradation rate of MB over TiO_2 sample firstly increased reaching maximum and then decreased gradually with the increase of Sm doping concentration. The photocatalytic activity of Sm-TiO_2 sample was the highest (97%) with n(Sm): n(Ti)=0.006, which was obviously better than that of pure TiO_2 sample (56.4%) under the same conditions.

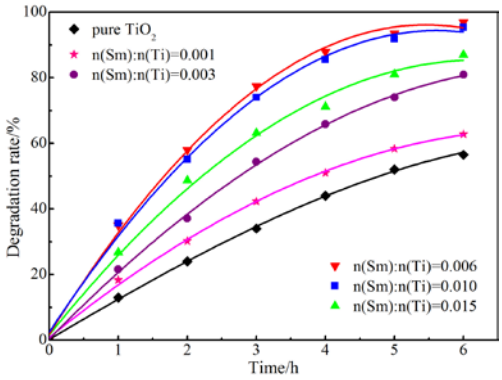

Figure 4. The degradation of MB over Sm-TiO_2 samples with different Sm doping concnrtration.

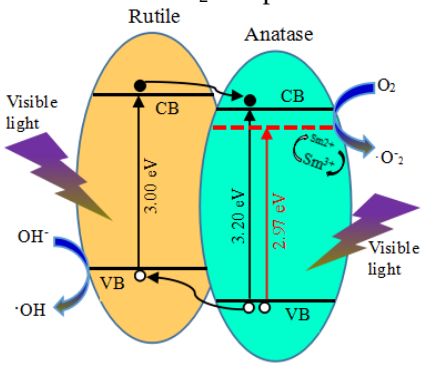

Figure 5. Schematic illustration of the reaction mechanism of photodegradation of MB over the Sm-TiO_2 samples.

The reasons for the influence of Sm doping on the photocatalytic enhancement of TiO_2 may be described as follows: (1) Sm-doping titanium dioxide is a mixture of rutile and anatase phases in proper proportion, which can form a strong heterojunction at the interface of the two phases and become a channel for electron transport. As shown in Figure 5, the photoinduced electron transfers to the conduction band of anatase phase induced by rutile phase with narrow band gap and the electron density on the surface of rutile phase decreases correspondingly. At the same time, the photogenerated hole produced by the anatase phase migrates to the valence band of the lower rutile phase. It is in this way. The photogenerated electron-hole pairs produced by the excitation of mixed phase TiO_2 migrate in opposite directions, respectively. Superoxide radicals ($\cdot O_2^-$) are formed by the reaction of photogenerated electron enriched on the surface of anatase phase with O_2 adsorbed on the surface of catalyst. Meanwhile, hydroxyl radicals (·OH) are formed by the reaction of photogenerated hole enriched on the surface of rutile phase with H_2O or OH^-adsorbed on the surface. It is precisely because these strong oxidative groups, such as $\cdot O_2^-$ and ·OH, oxidize and decompose MB organic matter into inorganic molecules. (2) The doping of rare earth metal ions changes the state of the energy level of TiO_2. A new impurity energy level formed by doping lies between the conduction band bottom and the valence band top. The effect of impurity energy level is equivalent to reducing the band gap width and expanding the absorption wavelength of light [21]. XPS analysis showed that Sm^{3+} and Sm^{2+} species existed on the surface of the catalyst after Sm-TiO_2. The empty orbits of Sm^{3+} could be used as electron transport channels to transport photogenerated electron, but Sm^{2+} species with high activity easily lost electrons. The trapped elcctron were transferred to the MB molecules adsorbed on the catalyst surface again. That is accelerating the electron transport. The transfer speed effectively reduces the recombination probability of photogenerated electron-hole pairs. However, excessive Sm doping concentration may be saturated in the TiO_2 lattice and precipitate and adhere to the surface of the catalyst, thus affecting the photocatalytic reaction of TiO_2 [22]. Some Sm ions even evolve into composite centers of photogenerated electron-hole pairs. That may result in the recombination of photogenerated electron-hole pairs to decrease the photocatalytic performance of TiO_2. Therefore, the

appropriate Sm doping amount contributes to the composition of rutile and anatase mixed phase, and the nano-TiO_2 has the best performance.

4. Conclusions

The samarium appeared two kinds of Sm^{3+} and Sm^{2+} species on the surface of TiO_2 after Sm doping. Rare earth Sm ion doping is beneficial to increase the hydroxyl content on the surface of TiO_2, inhibit the transformation from anatase phase to rutile phase, and refine the grain size. Appropriate samarium doping can promote the formation of mixed phase of rutile and anatase in proper proportion, effectively reduce the recombination rate of photogenerated electron-hole pairs, enlarge the wavelength range of absorption spectrum, and improve the photocatalytic performance of TiO_2. When the calcination temperature is 500 C and the doping amount is n(Sm):When n(Ti) = 0.006, the photocatalytic activity of Sm-TiO_2 was the highest, and the degradation rate of MB was 97% in 6 h under ordinary fluorescent lamp, which was significantly higher than that of pure TiO_2 under the same conditions 56.4%.

5. Acknowledgements

The work was supported by Sichuan Science and Technology Program(2019YFG0274), the Natural Science Foundation of the Department of Education of Sichuan Province(17ZB0227), and the Open Fund of Yunnan Key Laboratory for Micro/nano Materials & Technology(KF2015005).

6. References

[1] Yan N N, Zhu Z Q, Zhang J, Zhao Z Y and Liu Q J 2012 *Mater. Res. Bull.* **47** 1869
[2] Lee H J, Bang J, Park J, Kim S and Park S M 2010 *Chem. Mater.* **22** 790
[3] Conesa J C 2013 *Catalysis Today* **208** 11
[4] Schneider J, Matsuoka M, Takeuchi M, Zhang J, Horiuchi Y, Anpo M and Bahnemann D W 2014 *Chem. Rev.* **114** 986
[5] Wang Z M, Liu B, Xie Z X, Li Y M, Shen Z Y and Zuo J L 2016 *J. Synth. Cryst.* **45** 229
[6] Huang F P, Zhang S, Wang S, Li C X and Liu C 2015 *Mater. Rep.* **29** 6
[7] Joanna R, Tomasz G, Janusz W S, Wojciech L and Adriana Z 2014 *Appl. Surf. Sci.* **307** 333
[8] Elbahy Z M, Ismail A A and Mohamed R M 2009 *J. Hazard. Mater.* **166** 138
[9] Stengl V, Bakardjieva S and Murafa N 2009 *Mater. Chem. Phys.* **114** 217
[10] Xiao Q, Si Z C, Zhang J, Xiao C and Tan X 2008 *J. Hazard. Mater.* **150** 62
[11] Eskandarloo H, Badiei A, Behnajady M A and Ziarani G M 2015 *Ultrason. Sonochem.* **26** 281
[12] Zhang Q H, Cao L and Guo J K 2000 *Appl. Catal. B* **26** 207
[13] Krunks M, Sildos I and Junolainen A 2012 *Appl. Surf. Sci.* **261** 735
[14] Yukimasa M and Sakae T 2007 *Appl. Surf. Sci.* **253** 3856
[15] Huang D G, Liao S J, Zhou W B, Quan S Q, Liu L and He Z J 2009 *J. Phys. Chem. Solids* **70** 853
[16] Tang J, Chen X, Liu Y, Gong W, Peng Z and Cai T 2013 *Solid State Sci.* **15** 129
[17] Myilsamy M, Murugesan V and Mahalakshmi M 2015 *J. Nanosci. Nanotechnol.* **15** 4664
[18] Furuta Y, Sung P 2015 *Chin. J. Catal.* **36** 1679
[19] Zhang L D and Mo C M 1995 *J. Nano-Struct. Mater.* **12** 831
[20] Konta R, Kato H, Kobayashib H and Kudo A 2003 *J. Phys. Chem. B* **107** 7970
[21] Liu Z, Guo B, Hong L and Jiang H 2005 *Phys. Chem. Solids* **66** 161
[22] Li F B, Li X Z and Hou M F 2004 *Appl. Catal. B* **48** 185